De Risi, A., *et al.*: High Efficiency Nanofluid Cooling System for Wind Turbines
THERMAL SCIENCE: Year 2014, Vol. 18, No. 2, pp. 543-554

543

# HIGH EFFICIENCY NANOFLUID COOLING SYSTEM FOR WIND TURBINES

by

## *Arturo DE RISI, Marco MILANESE, Gianpiero COLANGELO\*, and Domenico LAFORGIA*

Department of Engineering for Innovation, University of Salento, Lecce, Italy

*The efficiency of cooling system is critical for wind turbines, particularly during the hot season, when high temperatures could damage the electric generator and mechanical parts of the turbine. The cooling system proposed in this paper is able to increase the efficiency of heat transfer with the use of nanofluids and the wind turbine tower as a heat exchanger to dissipate waste heat in the environment. In this study the use of $Al_2O_3$-water nanofluids has been considered.*
*The results of this investigation appear encouraging because they have shown that the proposed new solution is able to assure highly efficient heat transfer and to limit thermal stresses on the electrical and mechanical components of wind turbines.*

Key words:   *wind turbine, nanofluid, cooling system*

## Introduction

Wind turbines, during operation, need to dissipate a large amount of heat, that, if not properly handled, might generate a temperature rise of the electrical and mechanical components and hence a further reduction of the overall efficiency. High temperatures also contribute to unexpected crash of the generators, which results in very expensive repair costs, particularly, for offshore power plants.

The cooling system of most wind turbines uses a forced flow of external air as heat transfer fluid. Such a flow directly cools the electrical and mechanical components or passes through an air/liquid heat exchanger, usually located on the top/back side of the nacelle. Manufacturers frequently use liquid cooled generators for turbines that operate in harsh environment. These types of generators are more compact than air-cooled ones and characterized by higher electrical efficiency, because of the better cooling and lower drag/friction losses.

The cooling system of most wind turbines usually requires high electric consumption to establish and sustain the airflow and, therefore, it increases the amount of dissipated heat. In addition, in the former case, the airflow can carry a large amount of dust, sand, salt, etc. within the nacelle, whereas in the late case the heat exchanger affects the airflow around the turbine, thus making more difficult its control.

* Corresponding author; e-mail: gianpiero.colangelo@unisalento.it

The rise in size of new generation wind turbines increases the heat to be dissipated to make the system work properly and efficiently. This work investigates the potential performance of an innovative cooling system, based on the use of the wind turbine tower as heat exchanger, here after referred to as wind tower heat exchanger (WTHE), coupled with the use of innovative heat transfer fluids, made of a mixture of water and nanoparticles, hereafter referred to as nanofluids.

This solution gives many advantages *vs*. the traditional cooling systems, under the point of view of the contaminations from moisture, salt, sand or other impurities into the nacelle. The new cooling technique can be used both for onshore and offshore wind turbines, but the advantages are more evident in the second case, due to the most severe operating conditions.

The use of nanofluids represents a possible solution to enhance the performance of water-cooled systems. Since 1904, Maxwell [1, 2] proposed to use high conductive particles suspended in a liquid to increase heat conductivity in common heat transfer fluids. Nanofluids are engineered colloidal suspensions of nanoparticles (1-100 nm) in a base heat transfer fluid such as water, organic or metal liquids, *etc*. Nanoparticles are typically made of chemically stable metals, metal oxides or carbon.

Solid particles have higher thermal conductivity than liquids and, therefore, this contributes to enhance heat transfer [3-5], momentum and mass transfer and reduces the sedimentation and erosion [6]. Such enhancement also depends on other factors, such as particles shape, volume fraction and thermal properties [7-11]. First studies investigated millimeter or micrometer particles sized, but, although revealed some enhancement, their dimensions caused quick sedimentations, abrasions and clogging [12, 13]. Nevertheless, such studies revealed a rise of 20% in thermal conductivity of nanofluids using 4 vol.% of CuO nanoparticles, with average diameter of 35 nm, dispersed in ethylene glycol. A similar behavior has been observed with $Al_2O_3$ nanoparticles [14] and better results were obtained by using Cu nanoparticles or carbon nanotubes [15, 16].
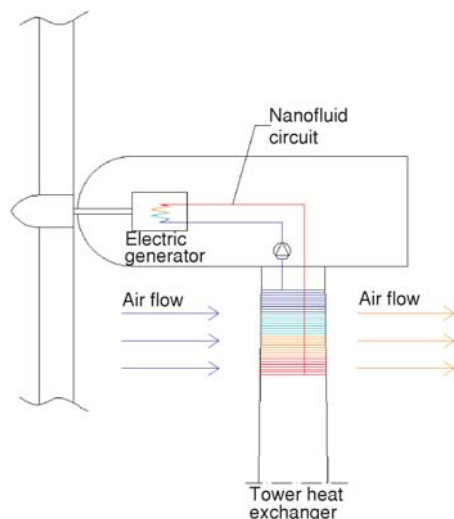


**Figure 1. Investigated cooling system configuration**

## Cooling system configuration

In the proposed cooling system the waste thermal load from electrical generators and mechanical components is dissipated through a WTHE, as fig. 1 schematically shows.

The WTHE is made of a spiral pipe, welded on the internal side of the tower. To reduce the height of tower involved in the heat transfer, each spire has been considered welded side by side one to each other. Besides, to improve heat transfer, a water-based nanofluid with $Al_2O_3$ nanoparticles is used in the WTHE circuit, instead of pure water.

In the present investigation, a 2 MW wind turbine has been studied, whose main characteristics are reported in tab. 1.

For more details, fig. 2 shows the electric generator efficiency curve and fig. 3 shows the relationship between the generator cooling water flow and the related pressure drop.

De Risi, A., *et al.*: High Efficiency Nanofluid Cooling System for Wind Turbines
THERMAL SCIENCE: Year 2014, Vol. 18, No. 2, pp. 543-554

545

**Table 1. Wind turbine dimensions**

| Parameter | Value |
|---|---|
| Maximum tower diameter | 4.15 m |
| Minimum tower diameter | 2.30 m |
| Tower height | 60.00 m |
| Rotor diameter | 76.00 m |

## Nanofluid characterization

### Nanoparticles characterization: measurements and models

Mixtures of base heat transfer fluid (water) with $Al_2O_3$, commercially available nanoparticles, have been tested in order to calculate nanofluids thermal properties for all the investigated operating conditions [3]. The main characteristics of the $Al_2O_3$ nanoparticles are reported next:

– Spherical shape
– Effective density: 3970 kg/m$^3$
– Mean size: 22.91 nm.

Thermal conductivity, $k_p$, and specific heat capacity, $c_p$, of $Al_2O_3$ nanoparticles have been calculated as function of temperature by means of the following polynomial correlations:

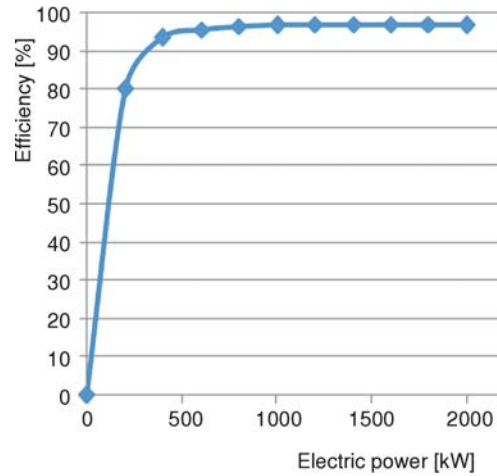$$k_p = a_1T^4 + a_2T^3 + a_3T^2 + a_4T + a_5 \quad (1)$$

$$c_p = b_1T^4 + b_2T^3 + b_3T^2 + b_4T + b_5 \quad (2)$$



**Figure 2. Electric efficiency of the 2 MW wind turbine generator**



**Figure 3. Experimental electric generator's cooling water flow volume as a function of pressure drop**

The value for all the constants $\alpha_i$ and $b_i$, reported in tab. 2, have been calculated by fitting experimental data, provided by the nanoparticles manufacturer and reported in figs. 4 and 5.
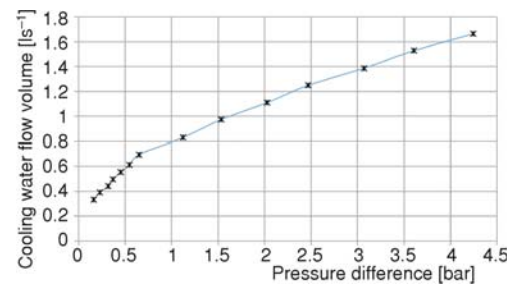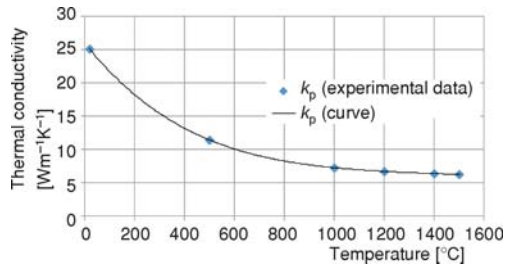
In order to predict the thermal conductivity and stability of nanofluid solid-fluid mixtures, many models have been developed, based on different theories [8, 17], but this is not the aim of this work and further considerations about this important issue will be developed in the next studies in order to optimize the thermal performance of the system.

**Table 2. Parameters for eqs. (1) and (2)**

| Parameter | Value | Parameter | Value |
|---|---|---|---|
| $\alpha_1$ | 3.564E-12 | $b_1$ | –2.003E-09 |
| $\alpha_2$ | 2.037E-08 | $b_2$ | 4.989E-06 |
| $\alpha_3$ | 4.521E-05 | $b_3$ | –4.783E-03 |
| $\alpha_4$ | –4.721E-02 | $b_4$ | 2.323 |
| $\alpha_5$ | 2.603E+01 | $b_5$ | 6.984E+02 |

546

De Risi, A., *et al*.: High Efficiency Nanofluid Cooling System for Wind Turbines
THERMAL SCIENCE: Year 2014, Vol. 18, No. 2, pp. 543-554
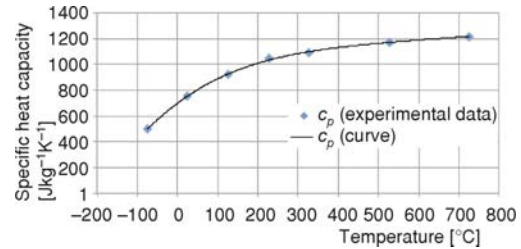
Figure 4. Thermal conductivity of nanoparticles



Figure 5. Specific heat of nanoparticles

*Nanofluids characterization: measurements and models*

The base fluid, used in the nanofluids samples, was demineralized water with non-ionic dispersant to stabilize the suspension. The nanofluid thermal conductivity was measured through an instrument based on the hot-wire technology [18], which is the standard method to measure thermal conductivity of non-metallic liquids, according to ASTM D 2717-95 [19].

**Table 3. Experimental data for nanofluid thermal conductivity for $Al_2O_3$ nanoparticles**

| Nanoparticle concentration [%] | Experimental thermal conductivity value [mWm$^{-1}$K$^{-1}$] |
|---|---|
| $\phi = 0\%$ | 606 |
| $\phi = 1\%$ | 622 |
| $\phi = 2\%$ | 635 |
| $\phi = 3\%$ | 647 |

To assure a perfect mixing between the nanoparticles and the base fluid, both liquid and solid phases were mixed for 60 minutes with a magnetic mixer. The suspension then was shacked in an ultrasonic sonicator, to break clusters of nanoparticles on an optimal level to assure good stability for a long time, without compromising thermal performance, according to other works [20]. Table 3 shows measured nanofluid thermal conductivity as function of $Al_2O_3$ nanoparticles volume fraction.

The investigated solid volume fractions were 0.0% (demineralized water without any particle inside), 1.0%, 2.0%, and 3.0%. Thermal conductivity was found to be directly proportional to volume fraction. For the reader convenience, a short summary of the mathematical models used for the calculation of nanofluids properties is reported next.

For particles concentration up to 3% thermal conductivity of the investigated nanofluids was taken by the measured data, whereas for concentration above 3% it has been calculated by means of Hamilton and Crosser model [21, 22] using eq. (3):

$$\frac{k_{nf}}{k_{bf}} = \frac{k_p + (n-1)k_{bf} - (n-1)\phi(k_{bf} - k_p)}{k_p + (n-1)k_{bf} - \phi(k_{bf} - k_p)} \tag{3}$$

where *n* is the shape factor.

The best fit of the experimental data of tab. 3 was achieved for a value of $n = 4.7$. According to Hamilton and Crosser [21] the shape factor is equal to 3 for spherical nanoparticles, therefore the used value indicates that particles agglomeration is present, even though all samples were treated with ultrasonic mixing. In the present investigation, all the mathematical models of nanofluids have been considered acceptable up to a nanoparticles volume concentration

equal to 10%. In this way, fig. 6 shows a comparison between experimental data and nanofluid thermal conductivity calculated according to eq. (3).

Other thermophysical properties, such as nanofluid density and nanofluid specific heat, have been calculated by using the models proposed by Buongiorno [23]:

$$\rho_{nf} = \phi \rho_p + (1 - \phi) \rho_{bf} \qquad (4)$$



**Figure 6. Thermal conductivity of nanofluids**

$$c_{nf} = \frac{\phi \rho_p c_p + (1 - \phi) \rho_{bf} c_{bf}}{\rho_{nf}} \qquad (5)$$

Several models have been proposed to calculate the convective heat transfer coefficient for nanofluids. Wang and Mujumdar [24] presented a complete review of existing models and available data about thermal conductivity and heat transfer characteristics of nanofluids. All the reported models are able to predict nanofluids thermal properties as function of the base fluid and nanoparticles type and concentration. However, all the reported models often give results very different one from each other, because they have been developed on a semi-empirical base and, to the knowledge of the authors, no universal correlation has been proposed in literature so far.

According to Mansour *et al*. [25], the experimental work by Pak and Cho [26], Li and Xuan [27], and Wen and Ding [28] have provided interesting insights into the hydrodynamic and thermal behavior of nanofluids in confined flows and have confirmed their superior thermal performance. These results led to empirical Nusselt number correlations for nanofluids with Cu, $TiO_2$ and $Al_2O_3$ particles, under laminar and turbulent flow conditions. However, none of the proposed correlations considered the effect of particles volume fraction. Xuan and Li [29] accounted for such a contribution by suggesting eq. (6) to calculate the Nusselt number for nanofluids as a function of particles concentration. Xuan and Li [29] derived their correlation from an experimental investigation on convective heat transfer of nanofluids flow in a tube under turbulent conditions, similar to the ones considered in the present study:

$$Nu_{nf} = 0.0059(1 + 7.6286 \varphi^{0.6886} Pe_{nf}^{0.001}) Re_{nf}^{0.9238} Pr_{nf}^{0.4} \qquad (6)$$

where Peclet number is calculated as $Pe_{nf} = D_p u_{nf}/\alpha_{nf}$, Prandtl number is calculated as $Pr_{nf} = c_{nf}\mu_{nf}/k_{nf}$, and $Re_{nf} = \rho_{nf}u_{nf}D_{pipe}/\mu_{nf}$.

In the above reported equations the effective dynamic viscosity is calculated using the polynomial curve fitting proposed by Wang *et al*. [30] and reported next:

$$\mu_{nf} = \mu_{bf}(123\phi^2 + 7.3\phi + 1) \qquad (7)$$

Finally, the heat transfer coefficients of nanofluids were evaluated by:

$$\frac{h_{nf}}{h_{bf}} = \frac{Nu_{nf}}{k_{nf}} \frac{k_{bf}}{Nu_{bf}} \qquad (8)$$

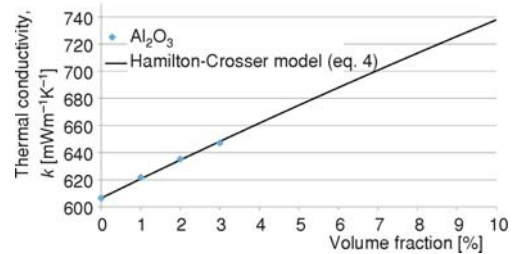where $h_{bf} = Nu_{bf}/k_{bf}D_{pipe}$ and $h_{nf} = Nu_{nf}/k_{nf}D_{pipe}$.

548

De Risi, A., *et al.*: High Efficiency Nanofluid Cooling System for Wind Turbines
THERMAL SCIENCE: Year 2014, Vol. 18, No. 2, pp. 543-554

The Dittus-Boelter correlation, reported in eq. (9), has been used to calculate the Nusselt number for the base fluid.

$$\text{Nu}_{bf} = 0.023\text{Re}^{0.8}\text{Pr}^{0.3} \tag{9}$$

## Numerical simulations

The heat transferred from the tower to the environment has been modeled by using the $\varepsilon$-NTU method, already used in other studies of high performance heat exchangers [31, 32], under the following hypothesis:

– the heat transfer between two neighboring pipes is neglected,
– it is assumed an external flow normal to the axis of the wind turbine pole, and
– the heat transfer takes place between the liquid phase, flowing in the pipe welded on the inner side of the pole, and the air outside the pole.

Under such conditions the wind tower results similar to a heat exchanger with a ratio of the heat capacity rates that approaches zero and therefore the WTHE efficiency can be calculated by:
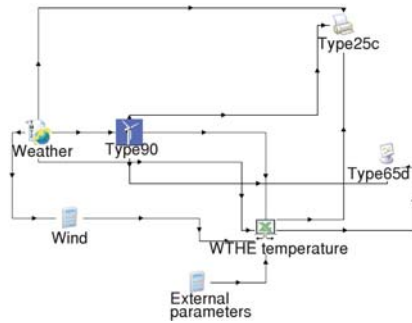
$$\varepsilon \approx 1 - e^{-\text{NTU}} \tag{10}$$

A parametric TRNSYS 16 model has been developed (see fig. 7) to simulate the overall performance of the proposed cooling system. Particularly, the 2 MW wind turbine was modeled by means of TRNSYS element Type90, which allowed to calculate the electric wind power ($P_e$) as a function of wind velocity. The waste heat from the electric generator has been evaluated according to eq. (11) and using the generator efficiency curve reported in fig. 2:

$$P_{th} = (1 - \eta_e)P_e \tag{11}$$

**Figure 7. TRNSYS model**

Several parameters, as the height of the WTHE, the nanoparticles volume fraction, and the mass flow rate of nanofluid were changed on 3 levels, as reported in tab. 4.

**Table 4. Values of the investigated parameters**

| Investigated parameters | Values | | |
|---|---|---|---|
| Height of WTHE [m] | 5 | 7.5 | 10 |
| Volume nanoparticles concentration [%] | 1 | 5 | 10 |
| Flow rate of nanofluid [l/s] | 0.5 | 1.0 | 2.0 |

Particularly, the values in tab. 4 have been set, bearing in mind the following considerations:

– the WTHE height has to be minimized, compatibly with the pole dimensions,
– the volume nanoparticles concentration is normally less than 5%, due to viscosity increment, but can be interesting to study the performance of the system in the case of higher concentrations, and
– the nanofluid flow rate has been set accordingly with wind turbine characteristics, as showed in fig. 3.

The results, that will be discussed next, are referred to meteorological data, acquired by the meteorological station number 163200 located in Brindisi, Italy, at the following coordinates N 40°39'00" E 17°57'10".

## Results and discussion

As first result, nanofluids can allow increasing the heat transfer coefficient significantly, accordingly with eq. (8), as reported in fig. 8. The ratio of the convective heat transfer coefficients rises with mass flow rate, due to the increased Reynolds number (as fig. 8 shows) and this irrespectively of nanoparticles concentration. The ratio of heat transfer coefficient curves, up to 5% in volume of nanoparticles, rises more than linearly, whereas for higher particles concentrations it leans towards a linear correlation. In addition, the heat transfer coefficient ratio for nanoparticles concentration equal to zero is not equal to one as it should be. This is due to the different values of the Nusselt number calculated with eq. (6) and (9) for nanofluids and water, respectively. Even with this discrepancy, the Xuan and Li correlation remains the best available in literature and all the other correlations [25, 29] yield greater errors in the calculations of the heat transfer coefficient as function of particles volume fraction.
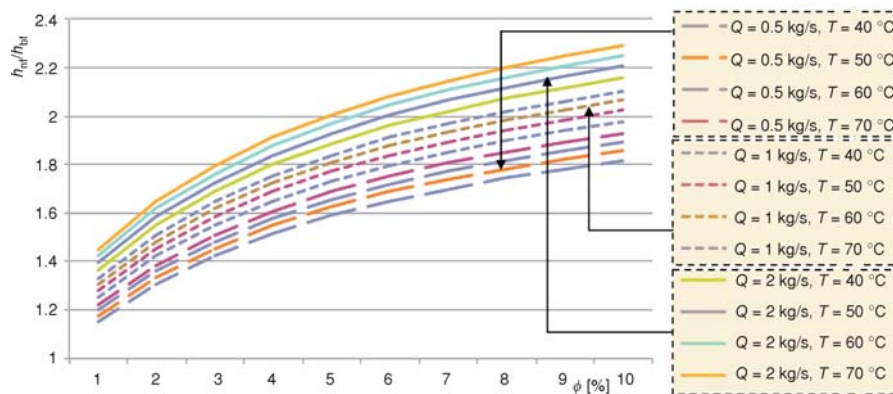


**Figure 8. Heat transfer ratio between nanofluid and base fluid**

The temperature dependence in the range between 40 °C and 70 °C is due to the change in material properties for both the base fluid and the nanoparticles. According to previous results, fig. 9 shows that the WTHE efficiency rises with nanoparticles concentration and mass flow rate, whereas the effect of nanofluid temperature in the range between 40 °C and 70 °C is negligible, in spite of the observed increment of the convective heat transfer coefficient. These results can be explained observing that the convective heat transfer coefficient of the nanofluid is generally two order of magnitude larger than that of the air on the outer surface of the wind turbine pole and, therefore, the overall heat transfer coefficient, $U$, given by eq. (12) is only marginally affected by a change of the convective heat transfer coefficient of the nanofluid side:

$$\frac{1}{U_{\text{nf}}} = \frac{1}{h_{\text{air}}} + \frac{(D_{\text{tower}} - 2s)\ln\left(\dfrac{D_{\text{tower}}}{D_{\text{tower}} - 2s}\right)}{2k_{\text{steel}}} + \frac{1}{h_{\text{nf}}} \qquad (12)$$
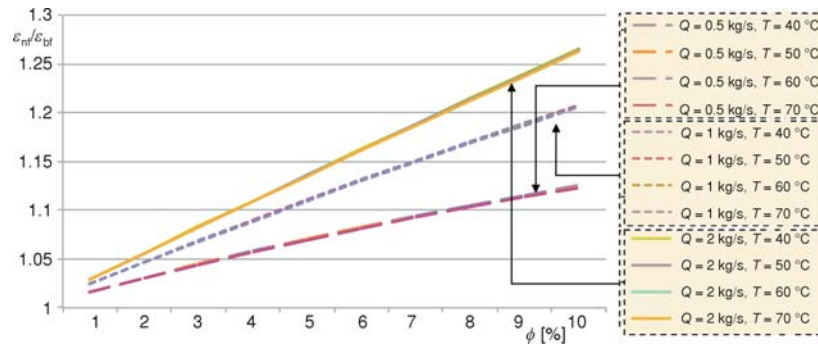
**Figure 9. WTHE efficiency as function of nanoparticles concentration**

Such considerations bring to the conclusion that the potential of nanofluids can be completely exploited in all the cases where a high heat flux can be achieved. For the system under investigation the highest heat fluxes are achieved for high value of the wind speed, when high thermal load has to be dissipated, and on the generator side, where the heat exchange surfaces are relatively small. Hot and windy days represent the most severe working conditions for the WTHE, because of both the high thermal output from the generator and the mechanical systems and the lower heat flux extracted by the air around the wind turbine pole. Such conditions were found in Brindisi, Italy, in the third and fourth week of July, therefore all the plots are referred to this period.
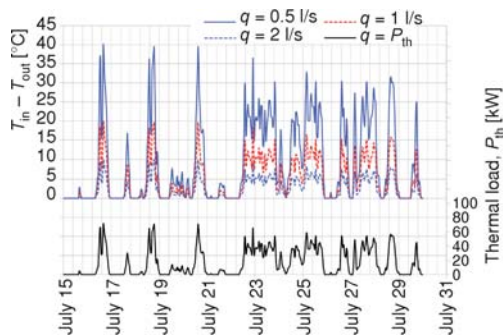


**Figure 10. Nanofluid temperature decrement between the inlet and the outlet of the WTHE for three nanofluid flow rates and a nanoparticle concentration of $Al_2O_3$ equal to 5 vol.% (top panel)**

In order to optimize the WTHE performance and to define the best combination of the parameters shown in tab. 4, several working conditions have been investigated. Particularly, the best value of nanofluid flow rate, among 0.5 l/s, 1 l/s, and 2 l/s, has been found by means of the nanofluid temperature variation between the WTHE inlet and outlet (this variation is opposite in sign with respect to the electric generator). In this way, fig. 10 reports the results for 3 nanofluid flow rates, equal to 0.5 l/s, 1.0 l/s, and 2.0 l/s, respectively, with a nanoparticles concentration of $Al_2O_3$ equal to 5 vol.%. Figure 10 shows that temperature variation in the WTHE, strictly follows the thermal load from the generator. This should not lead to the misleading conclusion that the system thermal inertia is negligible, but it is only due to the coarse time scale used for the graph. It was observed that peak temperature oscillations decrease with an opposite trend with respect to the flow rate, while the pumping power, as known, increases much more, being nearly proportional to the cubic power of the flow rate. The best compromise is achieved for a flow rate equal to 1 l/s, that assures a temperature variation between inlet and outlet from the WTHE lower than 20 °C. The height of the WTHE has been calculated on the base of the generator cooling specifications, which allowed maximum outlet temperature of the cooling fluid equal to 70 °C. Figure 11 shows the

De Risi, A., *et al.*: High Efficiency Nanofluid Cooling System for Wind Turbines
THERMAL SCIENCE: Year 2014, Vol. 18, No. 2, pp. 543-554

551

nanofluid outlet temperature from the electric generator. Data of fig. 11 are plotted for three different WTHE heights, using nanofluid with 5 vol.% of $Al_2O_3$ nanoparticles and a flow rate equal to 1 l/s.

As the curves of fig. 11 show, outlet temperature is always lower than 65 °C, only using a WTHE height equal to 10 m. The last parameter, that has been analyzed, is nanoparticles volume concentration. Particularly, the effect of nanoparticles concentration has been investigated following two approaches:

– analyzing the generator inlet temperature for three nanofluids concentration equal to 0 vol.% (water only), 5 vol.% and 10 vol.% of $Al_2O_3$ in water, respectively;
– calculating the maximum generator temperature, that cannot exceed the value of 90 °C.

The results of fig.12 show the curves relative to the most critical day in summer, whereas the results of fig. 13 refer to the coldest days in winter.

In the bottom panel of fig. 12 the thermal load to be dissipated is shown, the nanofluid inlet temperature of the generator panel is reported in the middle one and the temperature percentage difference of the nanofluid, with respect to the base fluid calculated by using eq. (13), is presented in the top panel:

$$\Delta T(\%) = \frac{T_{bf} - T_{nf}}{T_{bf}} \cdot 100 \qquad (13)$$

where $T_{bf}$ and $T_{nf}$ are the base fluid (water) and nanofluid temperature at the exit of the generator, respectively.



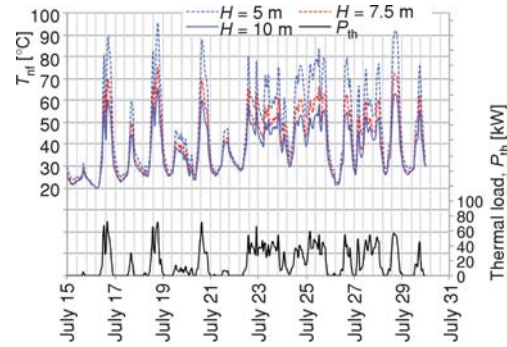**Figure 11. Nanofluid outlet temperature from the electric generator for three heights of the WTHE, nanoparticle concentration equal to 5 vol.% of $Al_2O_3$ and mass flow rate equal to 1 l/s (top panel)**



**Figure 12. Temperature percentage difference of the nanofluid with respect to the base fluid calculated by using eq. (13) (top panel). Mass flow rate equal to 1 l/s and WTHE height equal to 10 m (middle panel) in summer**

Figure 13 reports the same curves of fig. 12, but referred to winter. These charts reveal that by increasing particles concentration it is possible to reduce peak temperatures. Such reduction can be quantified up to 15% in summer and 34% in winter, using a nanofluid with 10 vol.% of $Al_2O_3$ and it is more relevant in winter, because of the higher achieved heat fluxes. To understand such a phenomenon it is important to notice that when WTHE is used, the overall heat transfer coefficient, given by eq. (12), is strongly limited by the low value of the convective heat transfer coefficient, hair, on the outer surface of the wind turbine pole, thus mitigating the effect of nanofluids. Vice versa, the advantage, that can be achieved by using nanofluids, is on the generator side, due to relatively small heat exchange surfaces. Figure 14 shows the maximum generator temperatures for 3 nanoparticles concentrations equal to 0 vol.% (water), 5 vol.% and 10 vol.% of $Al_2O_3$, mass flow rate equal to 1 l/s and WTHE height equal to 10 m.

552

De Risi, A., *et al.*: High Efficiency Nanofluid Cooling System for Wind Turbines
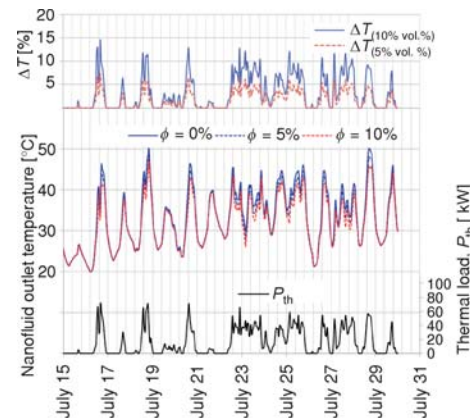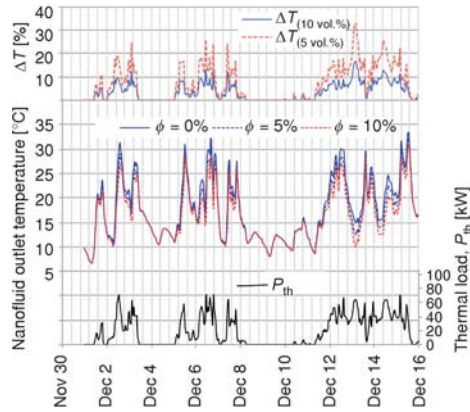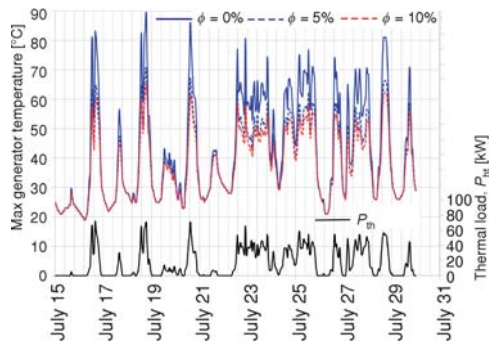THERMAL  SCIENCE: Year 2014, Vol. 18,  No. 2, pp. 543-554

**Figure 13. Temperature percentage difference of the nanofluid with respect to the base fluid calculated by using eq. (13) (top panel); mass flow rate equal to 1 l/s and WTHE height equal to 10 m (middle panel) in winter**



**Figure 14. Maximum generator temperature for three nanoparticles concentrations; mass flow rate equal to 1 l/s and WTHE height equal to 10 m (top panel) in summer**

As it is shown in fig. 14, nanofluids allow reducing significantly the maximum generator temperature. In fact, at peak thermal load, a nanoparticles concentration equal to 5 vol.% allows cutting the peak generator temperatures of about 20 °C. Therefore, the capability of nanofluids to extract a large amount of waste heat from the generator and from the mechanical apparatus can increase the performance of wind turbines, reducing thermal stress on the generator during wind blasts.

Nanofluids yield high heat transfer potentiality and thus it is expected that much smaller concentration of nanoparticles is required to achieve the same enhancements of larger particle suspensions. For this reason less material is needed so that the viscosity increase is smaller and the pumping power required is also reduced, if compared to larger particles. Under the point of view of pumping power, it increases almost ten times to double the heat transfer of traditional heat transfer fluids. For nanofluids it is different, because the heat transfer enhancement is higher and thus pumping energy can be saved if compared to traditional fluids at the same heat transfer rate. On the other hand, as reported in other studies [33-36], pressure drop could be negligible at low concentrations (under 3 vol.%), but it could be a big issue for high concentration or high Reynolds numbers. In these cases the use of nanofluids has to be evaluated with attention under the economic point of view, because of the risk of too high pumping power required by the system.

## Conclusions

In this work an innovative cooling system for wind turbine has been analyzed. In the proposed cooling system the thermal load, mainly from the electrical generator, is dissipated through the wind tower heat exchanger (WTHE), using nanofluids as heat transfer fluids.

Nanofluids, due to their high convective heat transfer coefficient, were found to improve the performance of the cooling system, especially when the environmental conditions allowed the establishment of high heat fluxes. Under steady-state condition the use of nanofluids increased the efficiency of the cooling system up to a maximum of 30%, depending on flow rate and particles concentration.

It was also found that for a wind turbine of 2 MW the height of the WTHE should not be lower than 10 m, with an $Al_2O_3$ nanoparticles concentration of 5 vol.%. In conclusion, the

cooling system of wind turbines, operating in harsh environment, is often a critical apparatus, in order to maintain the entire system working properly, and the proposed solution has been shown to be a very promising way to face this problem.

## Nomenclature

$c$ – specific heat capacity, $[\mathrm{Jkg^{-1}K^{-1}}]$
$D$ – diameter, [m]
$H$ – height, [m]
$h$ – heat transfer coefficient, $[\mathrm{Wm^{-2}K^{-1}}]$
$k$ – thermal conductivity, $[\mathrm{Wm^{-1}K^{-1}}]$
$n$ – nanoparticle shape factor
Nu – nusselt number
$P_e$ – electric power, [W]
Pe – Peclet number
Pr – Prandtl number
$P_{th}$ – thermal load to be dissipated, [W]
$Q$ – heat flux, $[\mathrm{Wm^{-1}}]$
$q$ – flow rate, $[\mathrm{m^3s^{-1}}]$
Re – Reynolds number
$s$ – thickness of the wind turbine tower, [m]
$T$ – temperature, [°C]
$t$ – time, [s]
$u$ – mean velocity, $[\mathrm{ms^{-1}}]$

*Greek symbols*

$\alpha$ – thermal diffusivity, $[\mathrm{m^2s^{-1}}]$
$\varepsilon$ – wind tower heat exchanger efficiency
$\phi$ – volume concentration
$\eta_e$ – generator electrical efficiency
$\mu$ – viscosity, [Pa·s]
$\rho$ – density, $[\mathrm{kgm^{-3}}]$

*Acronyms*

*NTU* – number of transfer unit
WTHE – wind tower heat exchanger

*Subscripts*

bf – base fluid
in – inlet
nf – nanofluid
np – nanoparticle
out – outlet

## References

[1] Xue, Q., Xu, W.-M., A Model of Thermal Conductivity of Nanofluids with Interfacial Shell, *Materials Chemistry and Physics, 90* (2005), 1-2, pp. 298-301
[2] Maxwell, J. C., A Treatise on Electricity and Magnetism, 2nd ed., Oxford University Press, Cambridge, UK, 1904
[3] Colangelo, G., *et al.*, Results of Experimental Investigations on the Heat Conductivity of Nanofluids Based on Diathermic Oil for High Temperature Applications, *Applied Energy, 97* (2012), Sept., pp. 828-833
[4] Colangelo, G., *et al.*, A New Solution for Reduced Sedimentation Flat Panel Solar Thermal Collector Using nanofluids, *Applied Energy, 111* (2013), Nov., pp. 80-93
[5] Hajian, R., *et al*., Experimental Study of Nanofluid Effects on the Thermal Performance with Response time of Heat Pipe, *Energy Conversion and Management, 56* (2012), 1, pp. 63-68
[6] Colangelo, G., *et al.*, A New Solar Panel Working with Nanofluids (in Italian), *Proceedings,* 66th ATI National Congress, 5-9 September, 2011, Rende, Italy, pp. 1-6
[7] Xuan, Y., Li, Q., Heat Transfer Enhancement of Nanofluids, *International Journal of Heat and Fluid Flow, 21* (2000), 1, pp. 58-64
[8] Keblinski, P., *et al*., Mechanism of Heat Flow in Suspensions of Nano-Sized Particles (Nanofluids), *International Journal of Heat and Mass Transfer, 45* (2002), 4, pp. 855-863
[9] Jang, S. P., Choi, S. U. S., Effect of Parameters on Nanofluids Thermal Conductivity, *Journal Heat Transfer, 129* (2007), 5, pp. 617-623
[10] Corcione, M., Empirical Correlating Equations for Predicting the Effective Thermal Conductivity and Dynamic Viscosity of Nanofluids, *Energy Conversion and Management, 52* (2011), 1, pp. 789-793
[11] Strandberg, R., Das, D. K., Influence of Temperature and Properties Variation on Nanofluids in Building Heating, *Energy Conversion and Management, 51* (2010), 7, pp. 1381-1390
[12] He, Y., *et al.*, Heat Transfer and Flow Behaviour of Aqueous Suspensions of $TiO_2$ Nanoparticles (Nanofluids) Flowing Upward through a Vertical Pipe, *International Journal of Heat and Mass Transfer, 50* (2007), 11-12, pp. 2272-2281

[13] Agwu Nnanna, A. G., Experimental Model of Temperature – Driven Nanofluid, *Journal Heat Transfer, 129* (2007), 6, pp. 697-704
[14] Lin, C.-Y., *et al*., Analysis of Suspension and Heat Transfer Characteristics of Al$_2$O$_3$ Nanofluids Prepared through Ultrasonic Vibration, *Applied Energy, 88* (2011), 12, pp. 4527-4533
[15] Xue, Q.-Z., Model for Effective Thermal Conductivity of Nanofluids, *Physics Letter A, 307* (2003), 6, pp. 313-317
[16] Hwang, Y., *et al*., Stability and Thermal Conductivity Characteristic of Nanofluids, *Thermochimica Acta, 455* (2007), 1-2, pp. 70-74
[17] Okeke, G., *et al*., Influence of Size and Temperature on the Phase Stability and Thermophysical Properties of Anatase TiO$_2$ Nanoparticles: Molecular Dynamics Simulation, *Journal of Nanoparticle Research, 15* (2013), 4, pp. 1584-1592
[18] Franco, A., An Apparatus for the Routine Measurement of Thermal Conductivity of Materials for Building Application Based on a Hot – Wire Method, *Applied Thermal Energy, 27* (2007), 14-15, pp. 2495-2504
[19] ***, ASTM D 2717 – 95, Standard Test Method for Thermal Conductivity of Liquids
[20] Okeke, G., *et al*., Computational Analysis of Factors Influencing Thermal Conductivity of Nanofluids, *Journal of Nanoparticle Research, 13* (2011), 1, pp. 6365-6375
[21] Hamilton, R. L., Crosser, O. K., Thermal Conductivity of Heterogeneous Two Component System, *I and EC Fundamentals, 1* (1962), 3, pp. 187-191
[22] Zhang, X., *et al.*, Effective Thermal Conductivity and Thermal Diffusivity of Nanofluids Containing Spherical and Cylindrical Nanoparticles, *Journal of Applied Physics, 100* (2006), 4, pp. 1-5
[23] Buongiorno, J., Convective Transport in Nanofluids, *Journal Heat Transfer, 128* (2006), 3, pp. 240-251
[24] Wang, X. Q., Mujumdar, A. S., Heat Transfer Characteristics of Nanofluids: a Review, *International Journal of Thermal Sciences, 46* (2007), 1, pp. 1-19
[25] Mansour, R. B., *et al*., Effects of Uncertainties in Physical Properties on Forced Convection heat Transfer with Nanofluid, *Applied Thermal Engineering, 27* (2007), 1, pp. 240-249
[26] Pak, B. C., Cho, Y. I., Hydrodynamic and Heat Transfer Study of Dispersed Fluids with Submicron Metallic Oxide Particles, *Experimental Heat Transfer, 11* (1998), 2, pp. 151-170
[27] Li, Q., Xuan, Y., Convective Heat Transfer Performances of Fluids with Nano Particles, *Proceedings,* 12th International Heat Transfer Conference, Grenoble, France, 2002, pp. 483-488
[28] Wen, D., Ding, Y., Experimental Investigation Into Convective Heat Transfer of nanofluids at the Entrance Region under Laminar Flow Conditions, *International Journal of Heat and Mass Transfer, 47* (2004), 24, pp. 5181-5188
[29] Xuan, Y., Li, Q., Investigation on Convective Heat Transfer and Flow Features of Nanofluids, *Journal of Heat Transfer, 125* (2003), 1, pp. 151-155
[30] Wang, X., *et al.*, Thermal Conductivity of Nanoparticles-Fluid Mixture, *J. Thermophys. Heat Transfer, 1*3 (1999), 4, pp. 474-480
[31] Colangelo, G., *et al*., Experimental Study of a Burner with High Temperature Heat Recovery System for TPV Applications, *Energy Conversion and Management, 47* (2006), 9-10, pp. 1192-1206
[32] Colangelo, G., *et al*., New Approaches to the Design of the Combustion System for Thermo Photovoltaic Applications, *Semiconductor Science and Technology ,18* (2003), 5, pp. S262-S269
[33] Xinyu Wu, *et al.*, Pressure Drop and Heat Transfer of Al$_2$O$_3$-H$_2$O Nano Fluids Through Silicon microchannels, *Journal Micromechanical Microengineering, 19* (2009), 105020
[34] Ziaei-Rad, M., Numerical Investigation of Pressure Drop and Heat Transfer in Developing Laminar and Turbulent Nanofluid Flows, *Physica Scripta*, T155 (2013), 014021
[35] Bayat, J., Nikseresht, A. H., Thermal Performance and Pressure Drop Analysis of Nano Fluids in Turbulent Forced Convective Flows, *International Journal of Thermal Sciences, 60* (2012), 1, pp. 236-243
[36] Bayat, J., Nikseresht, A. H., Investigation of the Different Base Fluid Effects on the Nano Fluids Heat Transfer and Pressure Drop, *Heat Mass Transfer, 47* (2011), 9, pp. 1089-1099